Supporting Information

Physical and chemical model of ion stability and movement within the dynamic and voltage-gated STM tip-surface tunneling junction

Brandon E. Hirsch, Kevin McDonald, Steven L. Tait, Amar H. Flood

Department of Chemistry, Indiana University,800 E. Kirkwood Avenue, Bloomington, IN 47405 (USA)

Email of corresponding authors: tait@indiana.edu, aflood@indiana.edu

S1. van der Waals forces of the surface

S2. Electrostatic forces of the surface

S3. van der Waals forces of the tip

S4. Electrostatic forces of the tip

S5. Density functional theory calculation

S6. Array of 25 molecules with the anion

S7. van der Waals forces of the molecule

S8. Electrostatics of the molecule

S9. Electric field between the tip and surface

S10. 2D contour plots

S11. α Phase assembly of ATO-C_{12}

S12. ATO-C_{12} α phase with no anions

S13. Line profiles of tip retractions

S14. ATO-C_{12} α phase with bias switching with no anions

S15. Energy-distance plots

S1. van der Waals forces of the surface

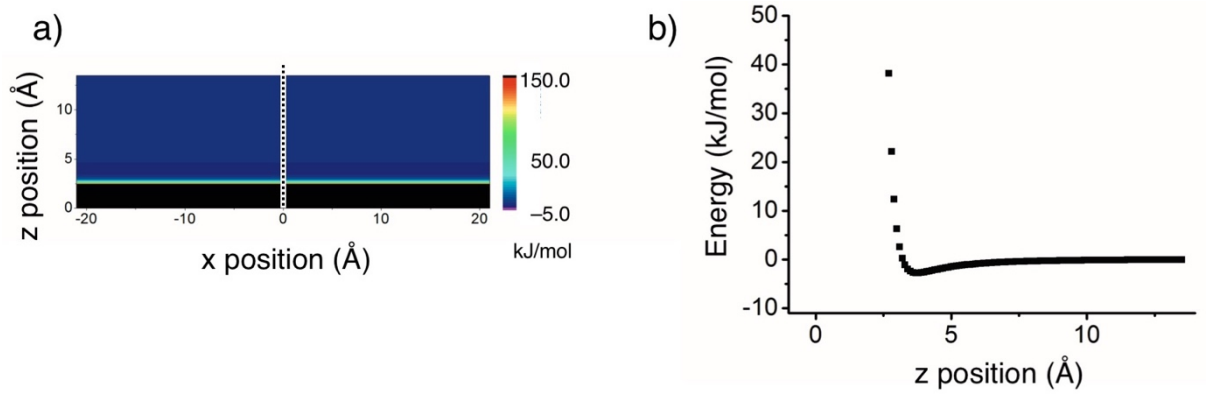

Figure S1. a) 2D contour plot of the modelled vdW forces between the bromide anion and the surface of graphite that was modelled as a semi-infinite plane. b) Potential energy plotted as a function of *z* position at the position $x = 0.0$ Å (shown in a) as a dotted line), which is the position of the anion binding pocket in the molecular receptor.

The vdW interactions with the HOPG surface were calculated based on a point interacting with a semi-infinite plane.[1] The energy is dependent on (z) the position of the anion above the surface:

$$V(z) = 4\varepsilon\left(\frac{\sigma^{12}}{z^{12}} - \frac{2\pi\rho\sigma^{6}}{12z^{3}}\right)$$

with ε and σ values of 0.382 kJ / mol and 3.6 Å, respectively. The density of atoms in the surface ρ was set to 0.114 $Å^{-3}$ based on the unit cell measurements for the HOPG surface.

S2. Electrostatic forces of the surface

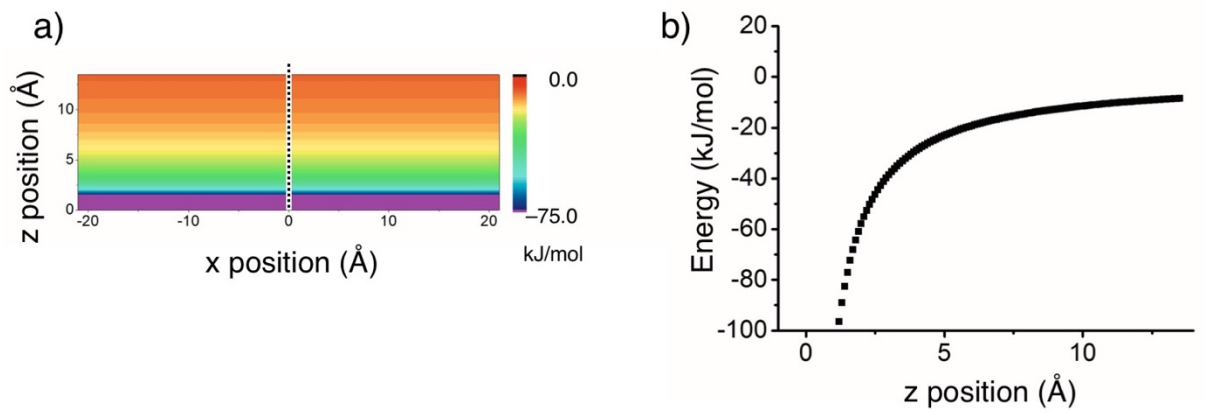

Figure S2. a) 2D contour plot of the modelled ES forces between the bromide anion and the surface of graphite that was modelled as an infinite plane. b) Plot of potential energy as a function of *z* position at *x* = 0.0 Å, as shown in a) using a dotted line.

The image charge model, was used to describe electrostatic interaction in this case of a bromide anion near the surface of HOPG. This interaction was calculated using the equation below:[2]

$$V(z) = \mathrm{c}\frac{q^2}{4\pi\varepsilon_0\varepsilon \cdot 2z}$$

with a scaling factor *c* taken as 0.95 to represent 95% the original Coulombic interaction in graphite[3] and *q* as the charge of the anion.

S3. van der Waals forces of the tip

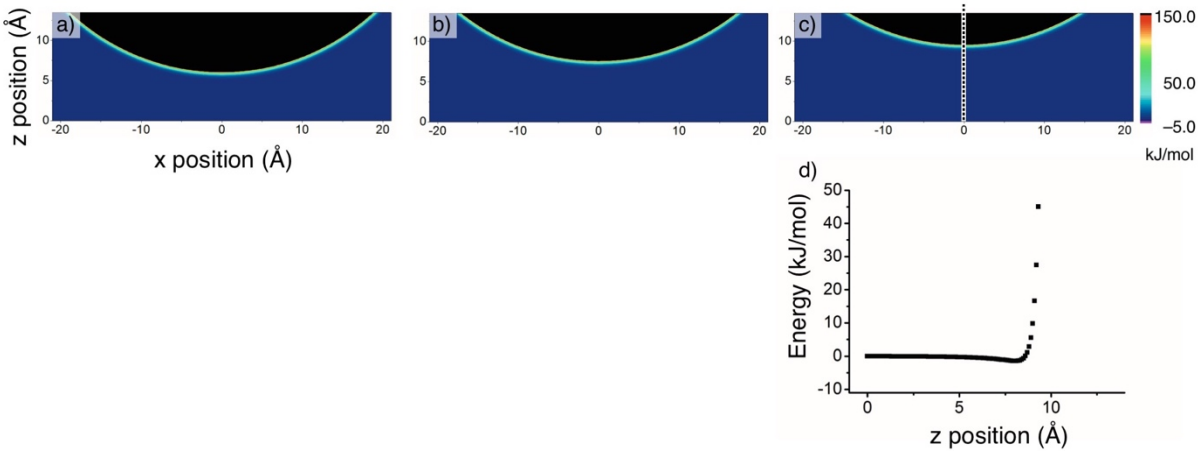

Figure S3. 2D contour plots of the modelled vdW forces between the bromide anion and the spherical tip. Three tip positions, a) z = 8.5 Å, b) z = 10.0 Å, c) z = 12.0 Å, are shown. d) Plot of potential energy as a function of z position at x = 0.0 Å, with a tip height z_{tip} = 12.0 Å as shown in c) using a dotted line.

The vdW interactions of the anion with the tip, modelled as a sphere of r_{tip} = 25 Å, were calculated based on a particle-sphere form of the Lennard-Jones (LJ) potential:[1]

$$V(d) = 4\varepsilon\left(\frac{\sigma^{12}}{d^{12}} - \frac{4}{3}\frac{r_{tip}^3\pi\sigma^6\rho}{(d+2r_{tip})^3 d^3}\right)$$

where d is the distance between the anion and the surface of the tip and ε and σ are vdW parameters with values of 0.41 kJ/ mol and 3.6 Å, respectively. The density of atoms in the tip ρ was calculated to be 0.083 Å^{-3} based on unit cell measurements for Pt metal.

S4. Electrostatic forces of the tip

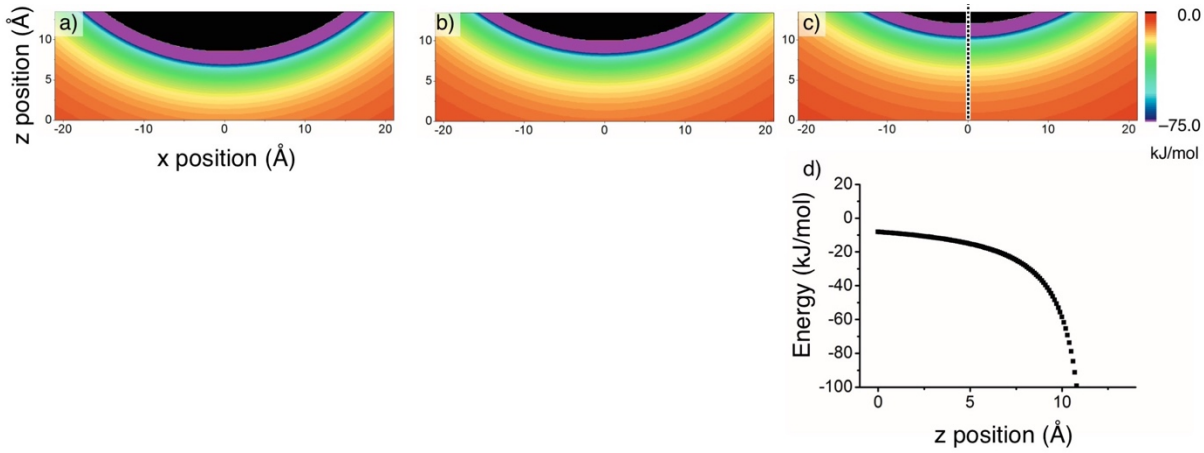

Figure S4. 2D contour plots of the modelled ES forces between the bromide anion and the spherical tip. Three tip positions, a) z = 8.5 Å, b) z = 10.0 Å, c) z = 12.0 Å, are shown. d) Plot of potential energy as a function of z position at x = 0.0 Å, with a tip height z_{tip} = 12.0 Å as shown in c) using a dotted line.

An image charge model was used to describe the anions interaction with the tip modelled as a sphere of r_{tip} (25 Å). This interaction was calculated using the equation below:[2]

$$V(\mathrm{z}, r) = \frac{q^2 r_{tip}}{4\pi\varepsilon_0 \varepsilon \cdot 2(r^2 - r_{tip}{}^2)}$$

Where r is the distance from the anion to the center of the tip and q is the charge on the anion.

S5. Density functional theory calculation

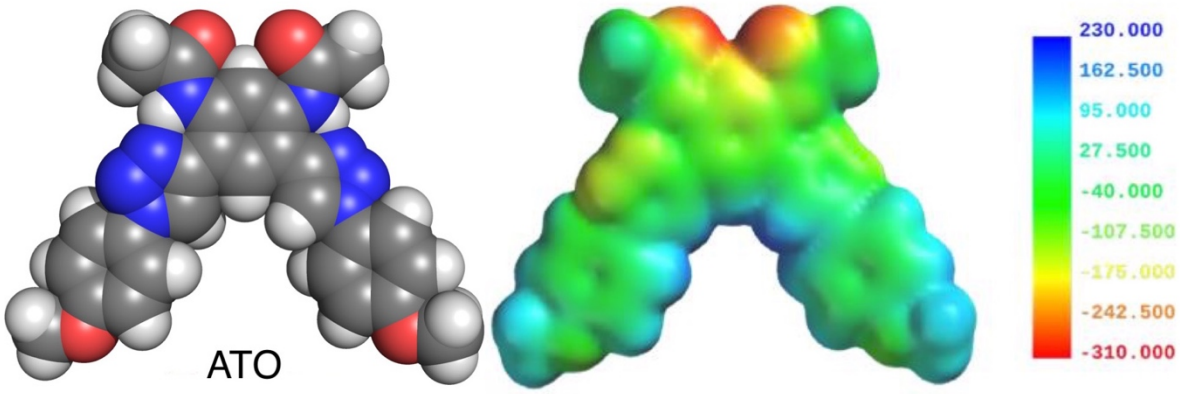

Figure S5. Geometry optimized structure (B3LYP/6-31G*) calculated with pentanoic acid solvent and electrostatic potential surface (ESP, B3LYP/6-31G*) for aryl-triazole oligomer (ATO) receptor with methyl truncation. The values for the ESP surfaces range from –310 (red) to +230 (blue) kJ / mol.

The geometry-optimized structures of anion receptor were determined using density functional theory (DFT) at the B3LYP/6-31G* level of theory with a pentanoic acid solvation model. Pentanoic acid was chosen because an octanoic acid solvent model was not available. It is, however, similar to octanoic acid; both are carboxylic acids and have similar dielectric constants of 3.3 and 2.8, respectively. The alkyl chains (both pentyl and C_{12}) were truncated to methyls for simplicity of the calculation.

S6. Array of 25 molecules with the anion

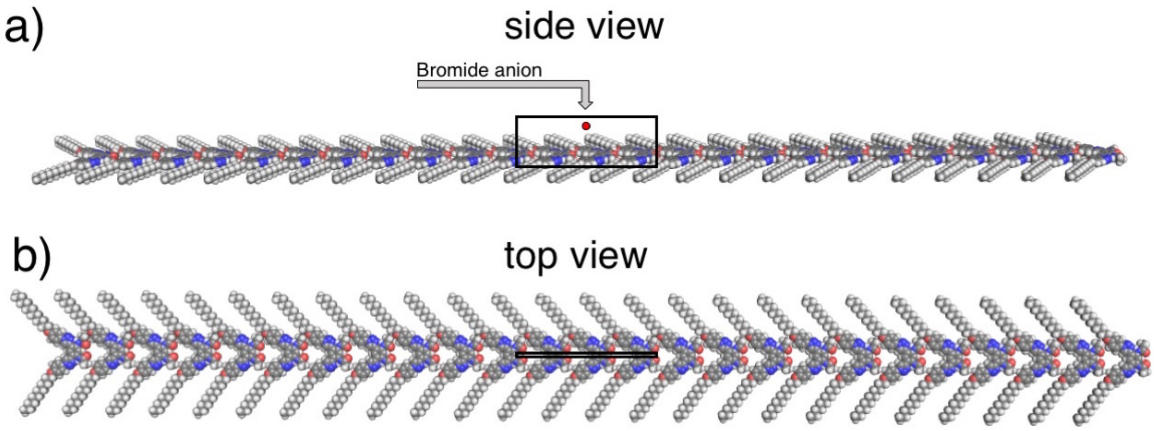

Figure S6. Schematic illustration of the modelled area viewed from the side a) and from the top b) of the interaction between the bromide anion with a row of twenty-five receptors by moving the anion along the *xz*-plane represented. An array of 25 molecules was used to minimize local variation in the potential energy of the surface due to molecular dipole moments of neighboring molecules, i.e., the local dipole potential with 25 molecules was relatively flat in the region studied.

S7. van der Waals of the molecule

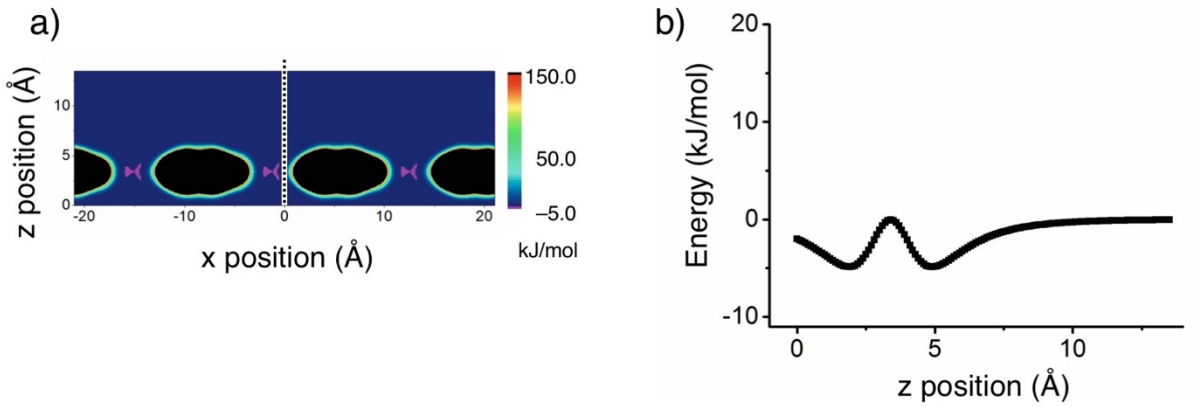

Figure S7. a) 2D contour plot of the modelled vdW forces between the bromide anion and the physisorbed ATO receptor molecules. b) Plot of potential energy as a function of *z* position at x = 0.0 Å, as shown with a dotted line in a). The vdW interaction between anion and molecular receptor was calculated pairwise using a Lennard-Jones 6-12 potential using atomic coordinates for each of 25 receptor molecules on the surface.

S8. Electrostatics of the molecule

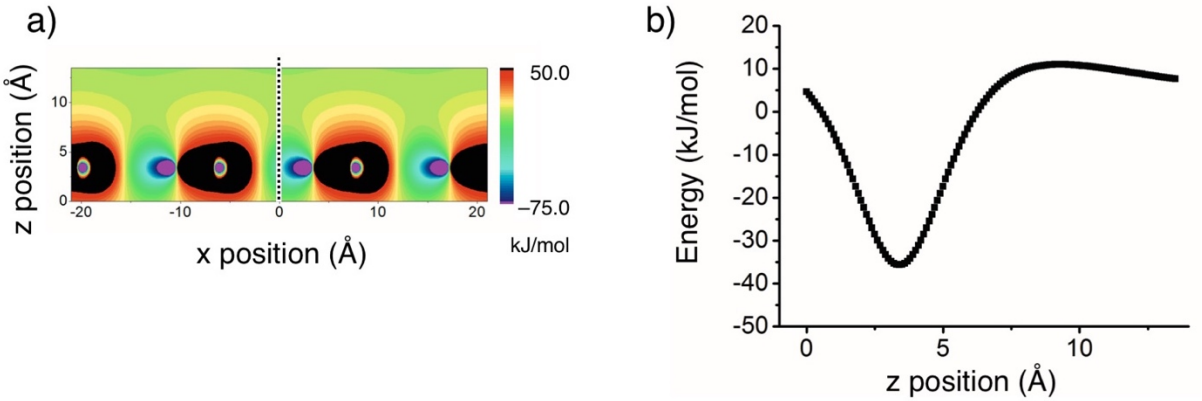

Figure S8. a) 2D contour plot of the modelled ES forces between the bromide anion and the physisorbed ATO receptor molecules. b) Plot of potential energy as a function of *z* position at $x = 0.0$ Å, as shown with a dotted line in a). The ES interaction between anion and molecular receptor was calculated pairwise using atomic coordinates and partial charges for each of 25 receptor molecules on the surface.

S9. Electric field between the tip and surface

To compute the electric field due to the STM bias, and in turn the potential energy of the anion within the field, the method of images was used for a charged sphere electrode near a conductive surface.[4] The potential energy felt by the anion, treated as a single negative point charge, at an arbitrary position between the tip (modeled as a sphere with radius 25 Å) and a semi-infinite plane is given by

$$\phi(r,z) = aV\sum_{i=0}^{\infty}\frac{\xi_i}{[(z-z_i)^2+r^2]^{1/2}} - \frac{\xi_i}{[(z+z_i)^2+r^2]^{1/2}}$$

where the potential $\phi(r,z)$ is found by a summing the image charges (ξ_i) at a particular bias V between the two objects. The 2D contour plots shown below demonstrate that the negatively charged bromide anion would migrate toward the surface when the surface is positively biased (Figure S9a-b, g). Alternatively at negative surface biases the anion will migrate toward the tip (Figure S9c-f, h).

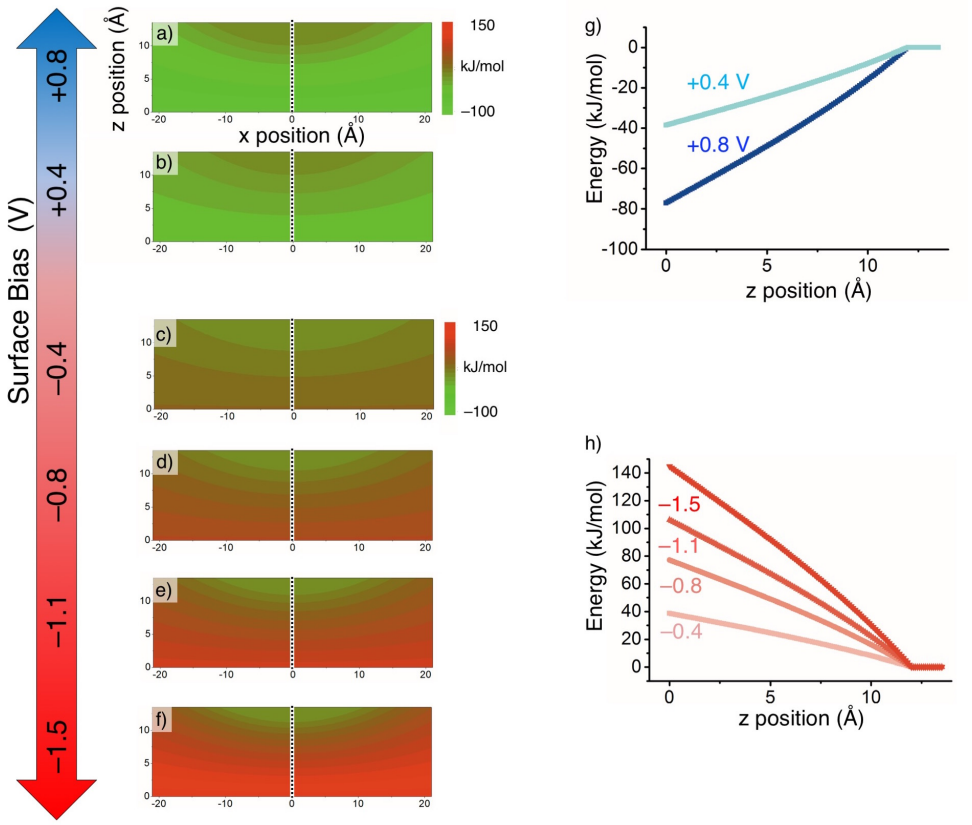

Figure S9. a-f) 2D contour plots series of the modelled interaction between the bromide anion and the electric field generated between the tip (z = 12.0 Å) and surface. The modelled surface biases are a) V_b = +0.8 V, b) V_b = +0.4 V, c) V_b = –0.4 V, d) V_b = –0.8 V, e) V_b = –1.1 V, and f) V_b = –1.5 V. g) z-nergy (kJ / mol) plot at the position x = 0.0 Å for the V_b = +0.8 V (deep blue) and V_b = +0.4 V (light blue). h) z-energy (kJ / mol) plot at the position x = 0.0 Å for the V_b = –0.4 V, –0.8 V, –1.1 V, –1.5 V in shades or red.

S10. Phase 2D contour plots

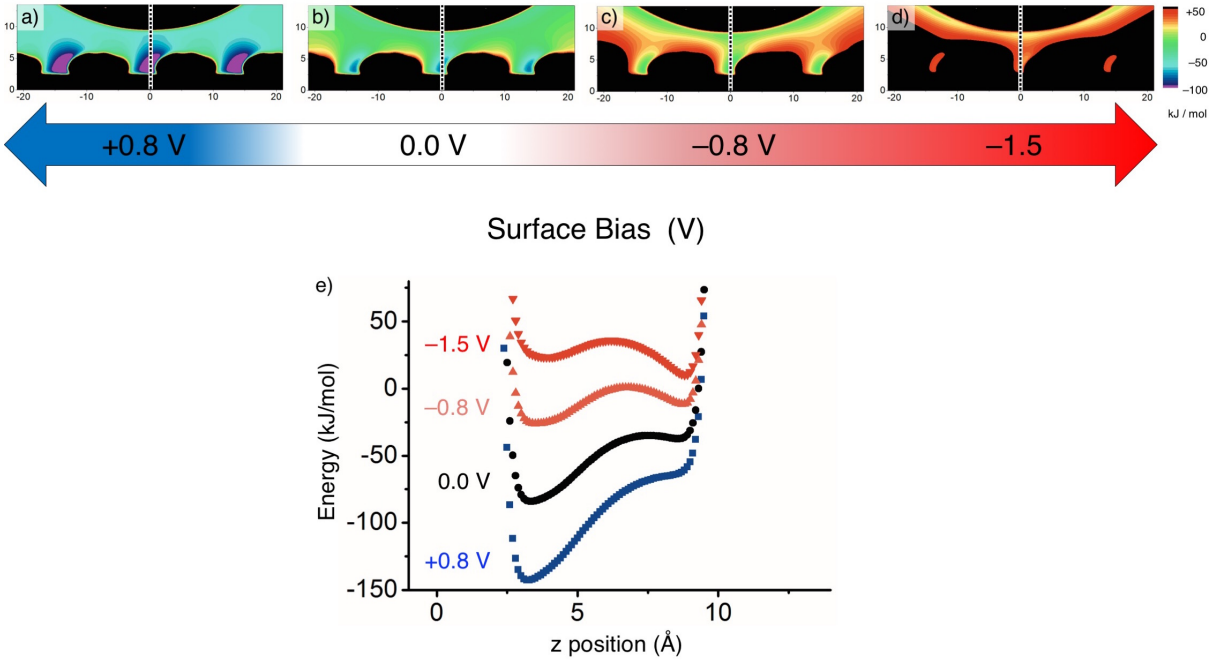

Figure S10. a-d) 2D contour plots series of the total interaction of the bromide anion in the tip-surface tunneling junction with the tip at z = 12.0 Å. The modelled surface biases are a) V_b = +0.8 V, b) V_b = 0.0 V, c) V_b = –0.8 V, and d) V_b = –1.5 V. e) z-energy (kJ / mol) plot at the position x = 0.0 Å for the all the surface biases plotted in a-d. Notice the drastic destabilization of the surface bound state at x = 3.4 Å when compared to the state that exists at the tip, x = 9.5 Å.

S11. α Phase assembly of ATO-C_{12}

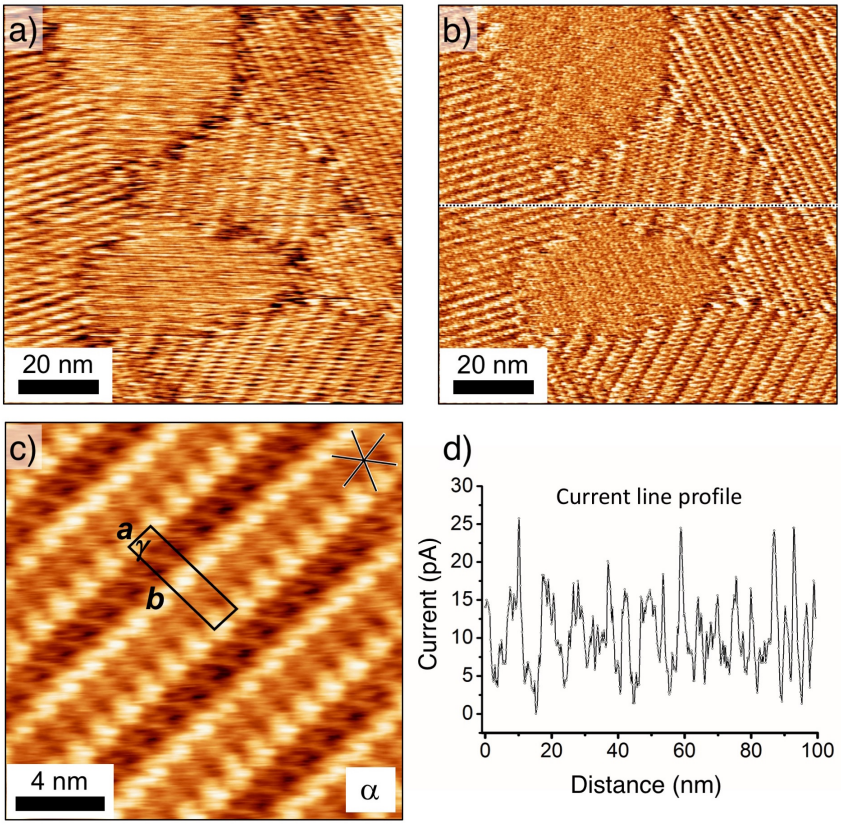

Figure S11. a) STM topography and b) current image the α phase assembly of ATO-C_{12} at the octanoic acid/graphite interface [ATO-C_{12}] = 1.0×10^{-4} M^{-1}. c) High-resolution STM image of the α phase assembly of ATO-C_{12}. Unit cell dimensions are a = 1.38 ±0.12 nm, b = 5.35 ±0.21 nm, and γ = 89.0 ±0.3º. Images were recorded at the octanoic acid/HOPG interface. (T = 23 ± 0.2 °C, I_t = 100 pA, V_b = –0.7 V). d) Line profile from the current image that appears in b). The current setpoint of 100 pA has already been subtracted off. The deviations 10–30 pA observed were observed as standard fluctuations for the free receptor.

S12. ATO-C_{12} α phase with no anions

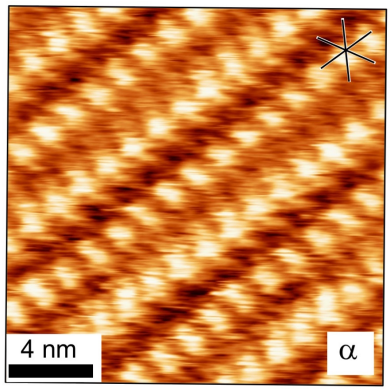

Figure S12. High-resolution STM image of the α phase assembly of ATO-C_{12} with a one-equivalent addition of the TBABr salt. No evidence of anion binding inside the ATO-C_{12} binding core could be observed. Image was recorded at the octanoic acid/HOPG interface. (T = 23 ± 0.2 °C, I_t = 100 pA, V_b = –0.432 V.

S13. Line profiles of tip retractions

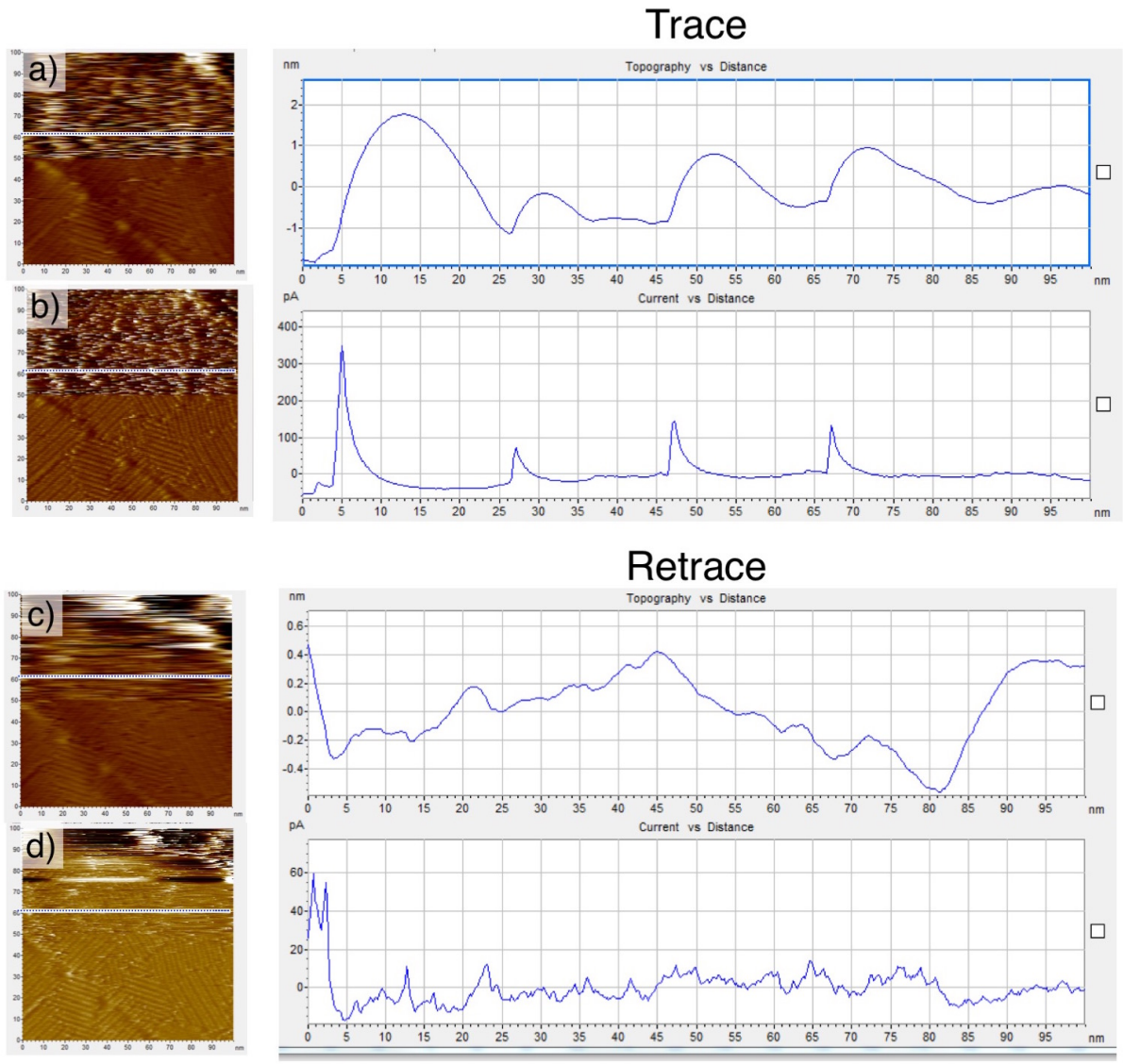

Figure S13. STM image comparison between the a) topography trace, b) current trace, c) topography retrace, and d) current trace for the self-assembly of ATO-C_{12} with one equivalent of TBABr added. Image was collected at the octanoic acid/HOPG interface. The bias was changed from V_b = –0.432 V at the top of the image to V_b = –0.832 V at the bottom of the image. Tunneling current was held consistent at I_t = 100 pA. Differences in the trace and retrace current images reveal asymmetry effects are likely involved in the tip anion ejection.

S14. ATO-C_{12} α phase with bias switching with no anions

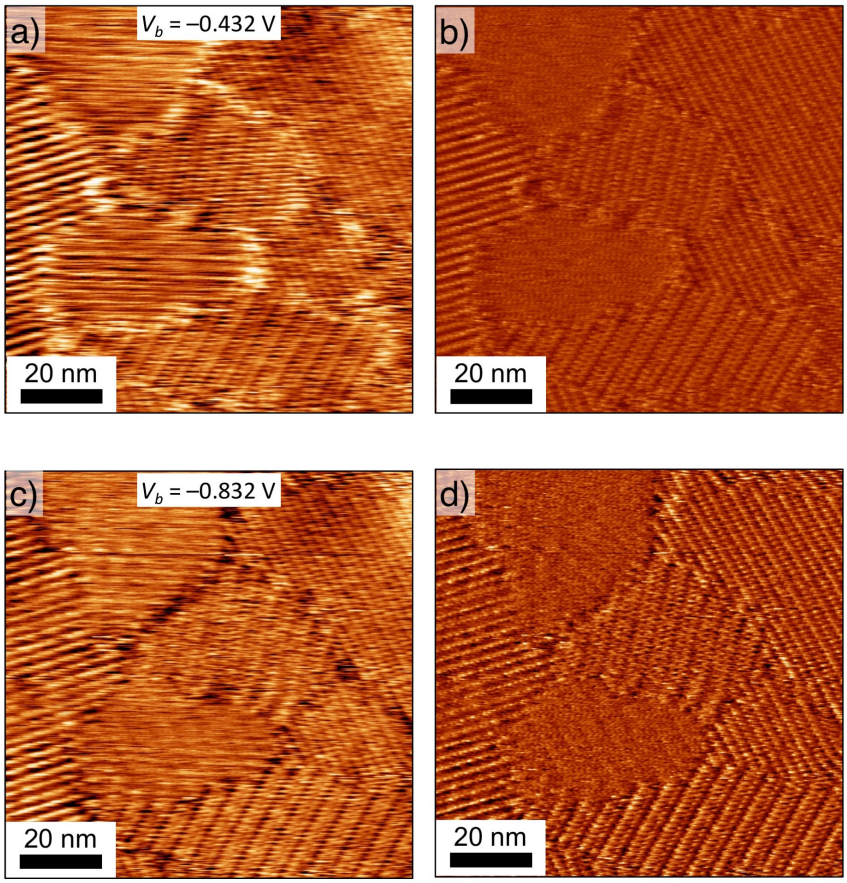

Figure S14. STM image comparison of the a) topography and b) current images of ATO-C_{12} when imaged at low bias V_b = –0.432 V at the octanoic acid/graphite interface. Similar resolution is also received in the c) topography and d) current images with larger negative surface biases V_b = –0.832 V. This demonstrates that the bias dependent clarity observed in when anions are added (Figures 5 and S13) is not the result of a change in the local density of states.

S15. Energy-distance plots

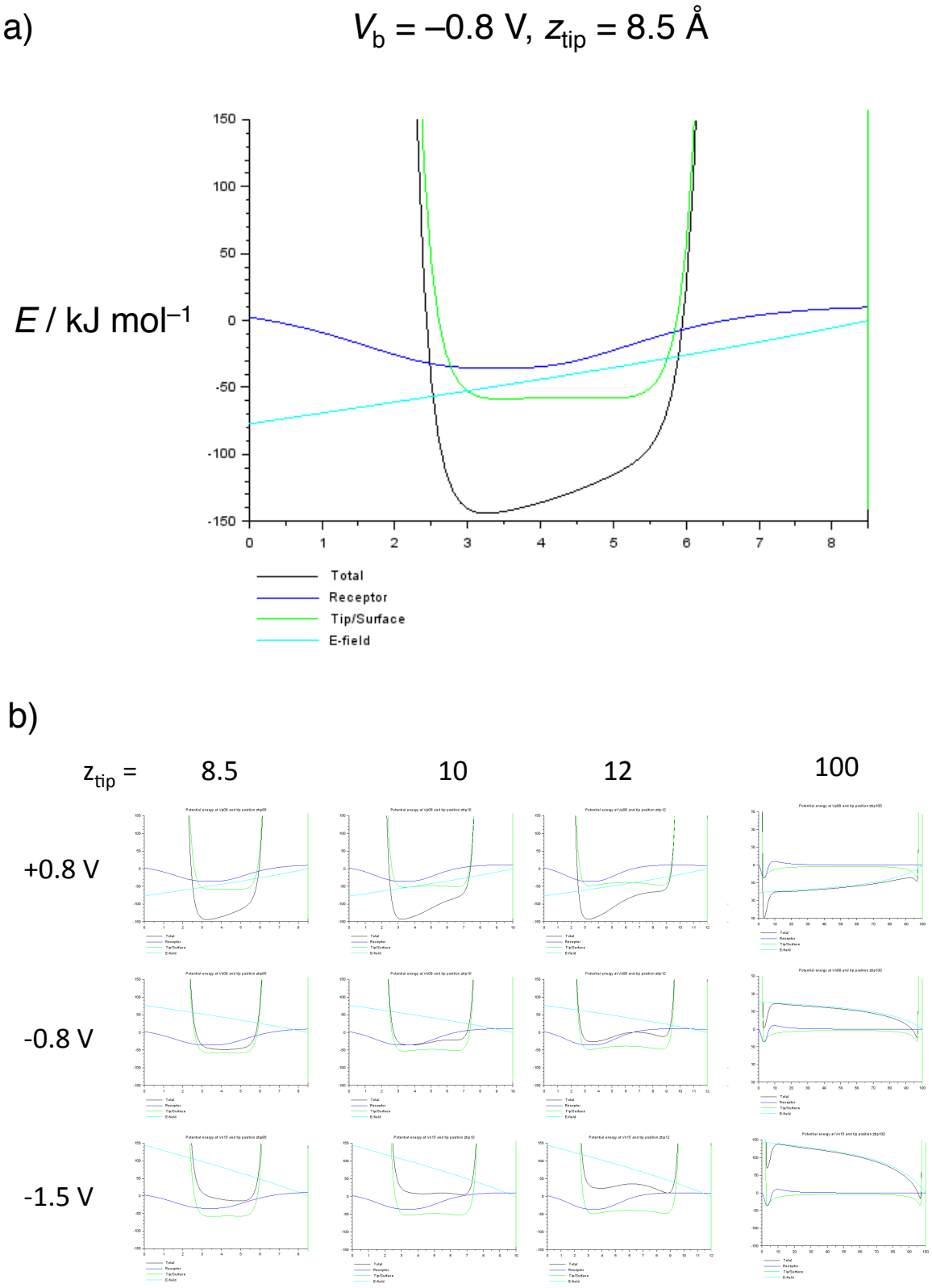

Figure S15. Plots of the energy of a bromide anion in the tip-surface junction as a function of bias (V_b) and z-distance between the tip and surface (z_{tip}) at the x = 0 Å position. a) Representative plot for V_b = –0.8 V and z_{tip} = 8.5 Å, and b) a series of plots for various biases and distances.

References

1. Israelachvili, J. N., *Intermolecular and Surface Forces*. 3rd ed.; Academic Press, Elsevier: Amsterdam, 2011.
2. Griffiths, D. J., *Introduction to electrodynamics*. 2nd Ed. ed.; Prentice-Hall, Inc.: Englewood Cliffs, New Jersey, 1989; p 124-125.
3. Jiang; Krauss, T. D.; Brus, L. E., *J. Phys. Chem. B* 2000, **104**, 11936-11941.
4. Dall'Agnol, F. F.; Mammana, V. P. *Revista Brasileira de Ensino de Física* 2009, **31**, 3503.1-3503.9.